JOURNAL OF MATERIALS SCIENCE 13 (1978) 1776–1780

Evaluation of microstructures associated with hardness indentations in InP

D. BRASEN
Bell Laboratories, Murray Hill, New Jersey 07974, USA

Microstructures associated with Knoop indentations on the (001) and (011) planes of single crystals of InP were evaluated by transmission electron microscopy (TEM). The results show that different $\{1\,1\,1\}\langle 1\,\bar{1}\,0\rangle$ slip systems are activated depending on the crystallographic direction along which the long axis of Knoop indentor is aligned. A simple explanation is developed which makes it possible to rationalize the observed slip systems and the hardness anisotropy of InP.

1. Introduction

Hardness anisotropy is a well known phenomenon and has been investigated for many b c c, f c c, and h c p crystals [1–5]. In a previous paper [6], this type of investigation has been extended to InP crystals which have the zinc-blende structure. It is observed that for InP the KHN (Knoop hardness number) varies with both the plane and direction of indentation.

A few attempts have been made to explain the observed hardness anisotropy of various crystals. Most of these studies are based on the work of Daniels and Dunn [1]. Basically they consider hardness to vary as an inverse function of a tensile force, F_T, acting parallel to the steepest slope of each facet of the Knoop indentor, and assume that the tendency to slip is limited to one slip plane per facet. For the purpose of analysis, the deformation was considered caused by small cylinders pulled in tension parallel to F_T. From this model they derive an "effective resolved shear stress" which in effect modifies the Schmid Law for slip by multiplying $F/A \cos\lambda \cos\phi$ by $\cos\psi$, where λ is the angle between F_T and the slip direction, ϕ is the angle between F_T and the normal to the slip plane and ψ is the angle between the direction in the slip plane perpendicular to the slip direction and the direction in the indentor–facet plane perpendicular to F_T. Their theory agrees fairly well with experimental results for cubic crystals [1, 3], but cannot explain the observed hardness anisotropy of h c p crystals. However, Feng and Elbaum [2] have been able to obtain a fairly close agreement with the experimental results for h c p Ti crystals by assuming a model similar to that of Daniels and Dunn, but using a force, F_N, which is normal to each facet of the Knoop indentor. Garfinkel and Garlick [4], have disputed the above models, claiming that the actual mechanism of deformation is complicated by the complex stress state associated with indentor penetration. In addition, Chin *et al.* [5] have shown that in order to produce crack-free deformation in most cases it would be necessary for more than one slip system (generally five) to be activated. Also, Wonsiewicz and Chin [7] have attempted to explain hardness anisotropy by assuming slip on five or more systems.

Hill and Rowcliff [8] have examined, by TEM, the details of plastic deformation processes around hardness indentations in Si. Unfortunately, they used a Vickers indentor, which gave inconclusive results as far as hardness anisotropy is concerned.

This paper will attempt to show that, with the aid of substructural details associated with hardness indentations in InP, it is possible to explain many features of the observed hardness anisotropy. InP was used because of the previous work done on it, and the fact that the zinc-blende structure has been found so far to exhibit only $\{1\,1\,1\}\langle 1\,\bar{1}\,0\rangle$ slip.

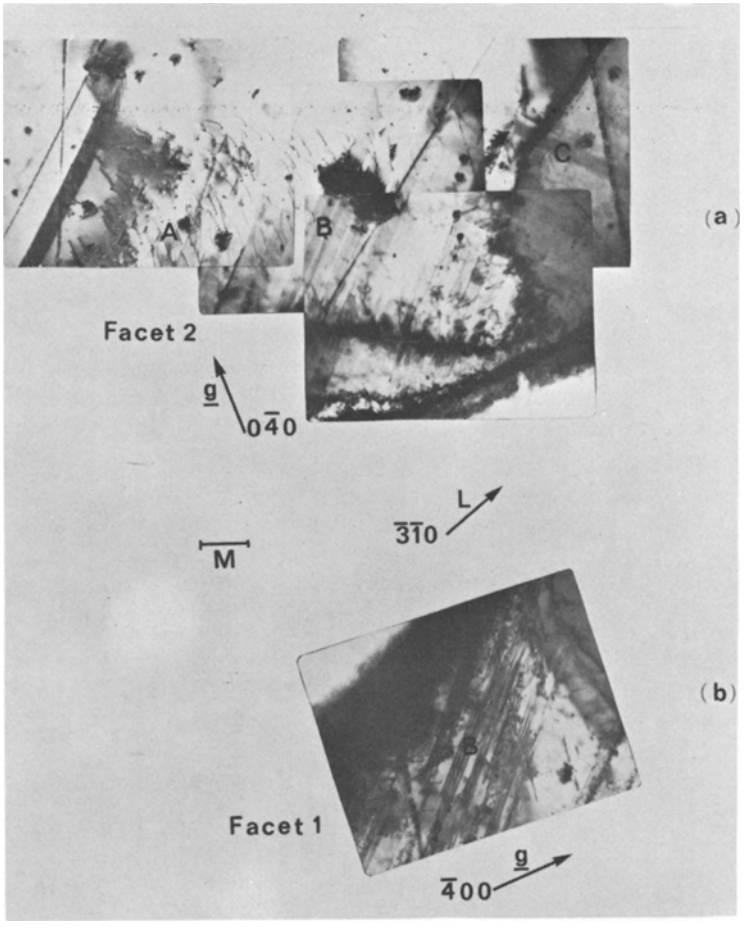

Figure 1 Electron micrographs of a portion of the area around a Knoop indentation in the (001) plane. L is pointing in the direction of the long axis of indentation. (a) Area around facet 2 using $0\bar{4}0$ reflection. (b) Area around facet 1 using $\bar{4}00$ reflection. Marker M represents 1 μm.

2. Experimental

Single crystals of InP were prepared for indentation on the (001) and (011) planes as described in the previous paper [6]. All indentations were made using a Kentron Microhardness Tester equipped with a Knoop diamond indentor and a calibrated eyepiece. All tests were standardized by using a 50 g load and completing each indentation within 20 sec. Indentation lengths were measured at a magnification of × 500.

After indenting, the backs of the samples were ground down to 0.010 in. using 600 grit SiC, and finally polished with Syton to remove the worked surface. Discs 3 mm in diameter containing the indentations were then cut out using an ultrasonic cutter. Next, the discs were thinned down for electron microscopy from the back, while protecting the indented surface, by polishing them in a solution of 2% Br in methanol. This part of the procedure was tedious because the discs with indentations on the (001) planes had a great tendency to cleave in the ⟨110⟩ directions, while the discs with indentations in the (011) plane had a tendency not to leave any thin areas before holes developed as the samples were etched. Because of these problems, the only samples that were successfully prepared were on the (001) plane with the long axis of the Knoop indentor in the $[\bar{3}\bar{1}0]$ direction and on the (011) plane with the long axis in the $[0\bar{1}1]$ direction.

Thin foils were then examined in a JEM 200 electron microscope operating at 200 kV. The goniometer stage on the TEM allowed tilting experiments up to 30°, while rotating up to 360°.

3. Results

In general, the networks of dislocations around the indentations showed a few characteristic defects. It was possible to identify these defects and classify them in an orderly manner. In all cases, in order to determine the Burgers vector of dislocations, the $\mathbf{g} \cdot \mathbf{b} = 0$ criterion was used where **g** is the operating reflection and **b** is the Burgers vector, while the $\mathbf{g} \cdot \mathbf{R} = 0$ or integer criterion, where **R** is a displace-

ment vector associated with a fault, was used to determine the slip plane of stacking faults.

Fig. 1 shows a composite of a portion of the area adjacent to two facets of the (001) $[\bar{3}\bar{1}0]$ Knoop indentation. Note the dislocations marked A lying in [010] direction. Contrast experiments show that these dislocations have a $\frac{1}{2}[011]$ or $\frac{1}{2}[0\bar{1}1]$ Burgers vector. The habit plane was determined by examining the stacking faults, B, whose traces lie along the [110] direction, and noting that for these faults $\mathbf{R} = \frac{1}{3}[1\bar{1}1]$ or $\frac{1}{3}[\bar{1}11]$. Thus, we see that a large stress must have been applied to the $(\bar{1}11)$ $[0\bar{1}1]$ and $(1\bar{1}1)$ [011] slip systems. Note that these faults appear to run from facet 1 to facet 2 or vice versa. Finally, the stacking faults marked C whose traces lie along the $[1\bar{1}0]$ direction were found to have $\mathbf{R} = \frac{1}{3}[111]$ or $\frac{1}{3}[11\bar{1}]$. Note that these faults are found only in facet 2 and not in facet 1.

Fig. 2 shows a portion of the $[0\bar{1}1]$ Knoop indentation on the (011) plane. The single most important feature here is the group of dislocations running in the $[21\bar{1}]$ direction of facet 2. Their Burgers vector was determined to be $\frac{1}{2}[10\bar{1}]$. This means that the slip plane must be either the (111) or $(1\bar{1}1)$, because these are the only planes which can contain the $\frac{1}{2}[10\bar{1}]$ Burgers vector. Upon closer examination, it can be seen that the ends of the dislocations lie in the $[0\bar{1}1]$ direction which outlines the trace of the (111) as the habit plane. This indicates that the principal stress was applied to the (111) $[10\bar{1}]$ slip system on this side of the indentor. The other side of the indentor, facet 1, shows dislocations running in the $[2\bar{1}1]$ direction. Using similar methods as before, it was determined that the Burgers vector of these dislocations is $\frac{1}{2}[\bar{1}10]$ and their habit plane is (111).

4. Discussion

As mentioned earlier, Daniels and Dunn's [1] effort to explain Knoop hardness anisotropy was based on the assumption that during the application of load, the indentor acts as a wedge imposing on the material a force, F_T, acting parallel to the steepest slope of each indentor facet, which causes some of the material to move to the surface around the indent. They, in effect, have ignored the force, F_N, acting normal to each indentor facet, which would have a tendency to compress the material. On the other hand, Feng and Elbaum [2] have proposed that F_N is the force to consider because "it seems to correspond more closely to reality". Since both models have shown some success in explaining experimental results, it may be assumed that both hypotheses are at least partially correct. Therefore it is proposed that the hardness anisotropy, within a given plane of indentation, may be governed by some linear combination of both forces, F_N and F_T, and that this resultant force, F_R, varies in magnitude and direction from material to material. It should be emphasized that this hypothesis is not to be considered as a complete representation of the mechanism for hardness anisotropy. A full description of the situation should also take into account other essentials such as work hardening, atomic packing, friction, ductility, and the interaction between different slip systems which are activated by different facets of the indentor. Nevertheless, this simple suggestion does reconcile two different

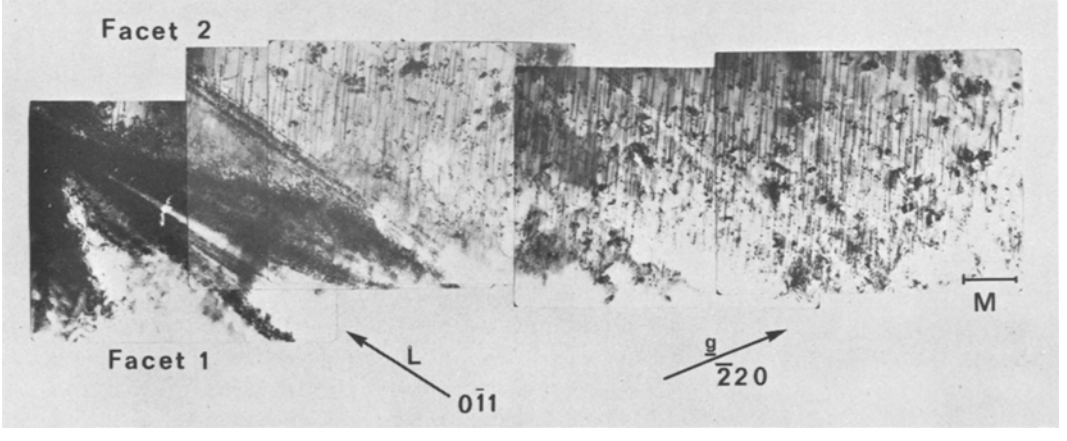

Figure 2 Electron micrographs showing a portion of a Knoop indentation on the (011) plane plus some of the area around facets 1 and 2. L is pointing in the direction of the long axis of indentation and Marker M represents 1 μm.

TABLE I Slip systems with corresponding NMRSS calculated for the four facets of the Knoop indentor with the long axis of indentation in the $[0\bar{1}1]$ and $[\bar{3}\bar{1}0]$ directions on the (011) and (001) planes respectively.

Plane	Direction	Facet 1		Facet 2		Facet 3		Facet 4	
		Slip system activated	NMRSS	Slip system activated	NMRSS	Slip system activated	NMRSS	Slip system activated	NMRSS
(001)	$[\bar{3}\bar{1}0]$	$(1\bar{1}1)\langle 011\rangle$ $(\bar{1}11)\langle 01\bar{1}\rangle$	−0.490	$(11\bar{1})\langle 011\rangle$ $(111)\langle 01\bar{1}\rangle$	0.467	$(1\bar{1}1)\langle 011\rangle$ $(\bar{1}11)\langle 01\bar{1}\rangle$	−0.490	$(11\bar{1})\langle 011\rangle$ $(111)\langle 01\bar{1}\rangle$	0.467
(011)	$[0\bar{1}1]$	$(111)\langle\bar{1}10\rangle$ $(\bar{1}11)\langle 101\rangle$	−0.440	$(111)\langle 10\bar{1}\rangle$ $(\bar{1}11)\langle\bar{1}\bar{1}0\rangle$	0.440	$(111)\langle\bar{1}10\rangle$ $(\bar{1}11)\langle 101\rangle$	−0.440	$(111)\langle 10\bar{1}\rangle$ $(\bar{1}11)\langle\bar{1}\bar{1}0\rangle$	0.440

approaches to the problem and also adds some insight as to how the different slip systems are activated.

In order to test this hypothesis for InP it was assumed that F_R would be parallel to the plane of indentation. However, to avoid the limiting constraints of Daniels and Dunn's model, the actual normalized resolved shear stress was calculated, on all possible slip systems, for each plane and direction that was checked for hardness in this paper and the previous one [6]. In this way, it was possible to look at all 12 slip systems for each facet of the indentor and thereby see if multiple slip per facet was theoretically possible.

Table I shows the slip systems with the maximum resolved shear stress calculated in this way, with F_R/A, where A is the area perpendicular to F_R, normalized to 1 (i.e., NMRSS for normalized maximum resolved shear stress), for the four facets of the Knoop indentor with the long axis of indentation in the $[0\bar{1}1]$ and $[\bar{3}\bar{1}0]$ directions. These indentations are on the (011) and (001) planes, respectively. Note that in the $[\bar{3}\bar{1}0]$ direction it is predicted that facets 1 and 3 should produce most of the slip by activating the $(1\bar{1}1)$ $[011]$ and $(\bar{1}11)$ $[0\bar{1}1]$ systems. Facets 2 and 4, on the other hand, may or may not activate slip on the (111) $[01\bar{1}]$ or $(11\bar{1})$ $[011]$ depending on how the slip systems interact with one another and with the indentor facets. Suppose, for example, that as the indentor is lowered and the critical stress for slip on facets 1 and 3 is reached, so that slip starts on the $(1\bar{1}1)$ $[011]$ and $(\bar{1}11)$ $[0\bar{1}1]$ due to the indentor facets. The stress would then increase in the area under facets 2 and 4. Thus, the indentor would be held up until the stress due to facets 2 and 4 would allow some slip on the $(11\bar{1})$ $[011]$ and/or (111) $[01\bar{1}]$. From this, it would be expected that many defects due to $(11\bar{1})$ $[011]$ and/or (111) $[01\bar{1}]$ slip should be seen, while some defects due to $(11\bar{1})$ $[011]$ and/or (111) $[01\bar{1}]$ slip may also be seen. Experimental evidence seems to bear this out.

When the indentor is in the $[0\bar{1}1]$ direction, Table I shows that the maximum resolved shear stress is equal on all four facets. Therefore, each facet should cause slip to occur on either or both of the slip systems with the maximum resolved shear stress for that facet. Fig. 2 shows that apparently once slip starts on a given system in each facet it continues on that system. Hence we see that in facet 1 there is mainly (111) $[\bar{1}10]$ slip, whereas in facet 2 there is mainly (111) $[10\bar{1}]$ slip.

In order to check out this model further, the Knoop hardness numbers which were measured and given in a previous paper [6], are compared in Table II to the NMRSS for a given direction of the long axis of indentation of the Knoop indentor on a given plane of indentation. Hardness values are tabulated in descending order with their corresponding NMRSS. The first feature to notice is

TABLE II Comparison of KHN with NMRSS for a given direction of the long axis of indentation of the Knoop indentor and a given plane of indentation.

Plane	Direction	KHN	NMRSS	Facet
(001)	$\langle 100\rangle$	430 ± 10	0.456	1, 2, 3, 4
	$\langle 110\rangle$	406 ± 11	0.456	1, 2, 3, 4
	$\langle 210\rangle$	370 ± 8	0.490	2
			0.467	1, 3
	$\langle 310\rangle$	367 ± 9	0.490	1, 3
			0.467	2, 4
(011)	$\langle 100\rangle$	399 ± 13	0.432	1, 2, 3, 4
	$\langle 1\bar{2}2\rangle$	353 ± 16	0.450	1, 3,
			0.363	2, 4
	$\langle 2\bar{1}1\rangle$	347 ± 14	0.354	2, 4
			0.335	1, 3
	$\langle 0\bar{1}1\rangle$	341 ± 15	0.440	1, 2, 3, 4
	$\langle 1\bar{1}1\rangle$	341 ± 15	0.440	1, 3
			0.379	2, 4
(111)	$\langle 3\bar{1}\bar{2}\rangle$	364 ± 11	0.467	2, 4
			0.429	1, 3
	$\langle 2\bar{1}\bar{1}\rangle$	359 ± 12	0.457	1, 2, 3, 4
	$\langle 10\bar{1}\rangle$	359 ± 11	0.457	1, 2, 3, 4

that, in general, as the hardness decreases in a given plane NMRSS increases, hence indicating some sort of inverse relationship as first proposed by Daniels and Dunn [1]. The actual relationship is probably very complex, especially where different facets of the indentor produce different NMRSS. The only exception to this general trend seems to be the hardness on the (0 1 1) plane, in the $[2\,\bar{1}\,1]$ direction. The reason for this is not yet clear. Another noticeable feature of Table II is that the model shows that there is apparently no relationship between NMRSS and their corresponding KHN for indentations in a given direction but in different planes. This is consistent with the fact that hardness anisotropy of InP is dependent on both the direction and plane of indentation [6]. Apparently, the hardness of each plane depends on other variables besides NMRSS, such as atomic packing.

5. Conclusions

The investigation of hardness indentations with the TEM has shown the following features:

(1) The microstructure of the (001) $[\bar{3}\bar{1}0]$ indentation shows most slip occurring on the $(\bar{1}\,1\,1)$ $[0\bar{1}1]$ and/or $(1\bar{1}1)$ [0 1 1] slip systems, while some slip does occur on the (1 1 1) and/or $(1\,1\,\bar{1})$ slip planes.

(2) The (0 1 1) $\langle 0\bar{1}1\rangle$ indentation shows that slip occurs on principally the (1 1 1) $[10\bar{1}]$ and the (1 1 1) $[\bar{1}10]$, depending on the facet.

By combining these facts with the KHN measured prviously for InP, it was possible to develop a simple model to explain many features which occur as a result of microhardness indentations, produced by a Knoop indentor, on InP at room temperature. This model shows that both the tensile force, as first proposed by Daniels and Dunn, and the compressive force identified by Feng and Elbaum, are important and can be combined to produce slip in a predictable way. Moreover, this theory is not limited to one slip plane per facet, as is the theory of Daniels and Dunn. However, this model has its limitations in that it only generally explains how hardness varies with direction and plane of indentation. In order to understand hardness anisotropy more completely much more work is needed.

Acknowledgements

The author wishes to thank S. Mahajan and G. Y. Chin for helpful discussions and constructive comments on this manuscript.

References

1. F. W. DANIELS and C. G. DUNN, *Trans. ASM* **41** (1949) 419.
2. C. FENG and C. ELBAUM, *Trans. Met. Soc. AIME* **212** (1958) 47.
3. C. A. BROOOKS, J. B. O'NEILL and B. A. W. REDFERN, *Proc. Roy. Soc. Lond.* **A322** (1971) 73.
4. M. GARFINKEL and R. G. GARLICK, *Trans. Met. Soc. AIME* **242** (1968).
5. G. Y. CHIN, M. L. GREEN, L. G. VAN UITERT and W. A. HARGREAVES, *J. Mater. Sci.* 8 (1973) 1421.
6. D. BRASEN, *ibid.* **11** (1976) 791-793.
7. B. C. WONSIEWICZ and G. Y. CHIN, Proceedings of the Symposium on the Science of Hardness Testing and its Research Applications (ASM, Detroit, 1971).
8. M. J. HILL and D. J. ROWCLIFF, *J. Mater. Sci.* 9 (1974) 1569.

Received 31 October and accepted 14 December 1977.